LETTER

doi:10.1038/nature21059

New CRISPR–Cas systems from uncultivated microbes

David Burstein[1]*, Lucas B. Harrington[2]*, Steven C. Strutt[2]*, Alexander J. Probst[1], Karthik Anantharaman[1], Brian C. Thomas[1], Jennifer A. Doudna[2,3,4,5,6] & Jillian F. Banfield[1,7]

CRISPR–Cas systems provide microbes with adaptive immunity by employing short DNA sequences, termed spacers, that guide Cas proteins to cleave foreign DNA[1,2]. Class 2 CRISPR–Cas systems are streamlined versions, in which a single RNA-bound Cas protein recognizes and cleaves target sequences[3,4]. The programmable nature of these minimal systems has enabled researchers to repurpose them into a versatile technology that is broadly revolutionizing biological and clinical research[5]. However, current CRISPR–Cas technologies are based solely on systems from isolated bacteria, leaving the vast majority of enzymes from organisms that have not been cultured untapped. Metagenomics, the sequencing of DNA extracted directly from natural microbial communities, provides access to the genetic material of a huge array of uncultivated organisms[6,7]. Here, using genome-resolved metagenomics, we identify a number of CRISPR–Cas systems, including the first reported Cas9 in the archaeal domain of life, to our knowledge. This divergent Cas9 protein was found in little-studied nanoarchaea as part of an active CRISPR–Cas system. In bacteria, we discovered two previously unknown systems, CRISPR–CasX and CRISPR–CasY, which are among the most compact systems yet discovered. Notably, all required functional components were identified by metagenomics, enabling validation of robust *in vivo* RNA-guided DNA interference activity in *Escherichia coli*. Interrogation of environmental microbial communities combined with *in vivo* experiments allows us to access an unprecedented diversity of genomes, the content of which will expand the repertoire of microbe-based biotechnologies.

We sought to identify previously unknown class 2 CRISPR–Cas systems in terabase-scale metagenomic datasets from groundwater, sediment, acid-mine drainage (AMD) biofilms, soil, infant gut, and other microbial communities. Our analyses targeted large uncharacterized genes proximal to a CRISPR array and *cas1*, the universal CRISPR integrase[8–10]. Among the 155 million protein-coding genes analysed, we identified the first Cas9 proteins in domain Archaea, and discovered two new CRISPR–Cas systems in uncultivated bacteria, which we refer to as CRISPR–CasX and CRISPR–CasY (Fig. 1). Both the archaeal Cas9 and CasY are encoded exclusively in the genomes of organisms from lineages with no known isolated representatives.

One of the hallmarks of CRISPR–Cas9 (type II) systems was their presumed presence only in the bacterial domain[3,11]. We were therefore surprised to discover Cas9 proteins encoded in genomes of the nanoarchaea '*Candidatus* Micrarchaeum acidiphilum ARMAN-1' and '*Candidatus* Parvarchaeum acidiphilum ARMAN-4'[12,13] in AMD metagenomic datasets (Extended Data Table 1 and Extended Data Fig. 1). These findings expand the occurrence of Cas9-containing CRISPR systems to another domain of life.

The CRISPR–Cas locus in ARMAN-1 includes large CRISPR arrays adjacent to the *cas1*, *cas2*, *cas4* and *cas9* genes. This system was found on highly similar contigs (an average nucleotide identity of 99.7% outside the CRISPR array) reconstructed independently from 16 different samples. We reconstructed numerous alternative ARMAN-1 CRISPR arrays with a largely conserved end (probably comprised of the oldest spacers) and a variable region into which many distinct spacers have been incorporated (Fig. 2a, Extended Data Fig. 2 and Supplementary Table 1). Given the polarity of the array, we predict that the approximately 200-bp region between the end of the Cas9 gene and the variable end of the array is likely to contain the leader sequence and transcriptional start site. On the basis of the hypervariability in spacer content, we conclude that the ARMAN-1 CRISPR–Cas9 system is active in the sampled populations. Phylogenetic analysis of Cas1 (Extended Data Fig. 3a) suggests that this archaeal CRISPR–Cas system does not clearly fall into any existing type II subtype. The presence of *cas4* affiliates it

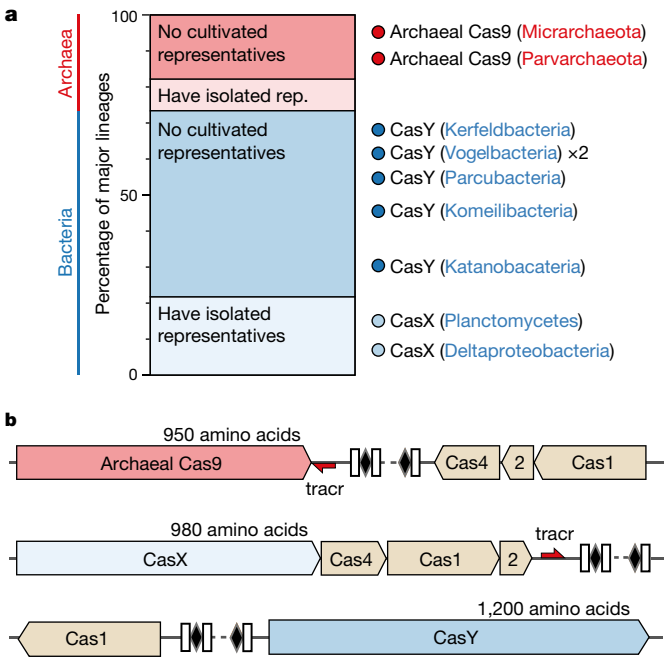

Figure 1 | CRISPR–Cas systems identified in uncultivated organisms. **a**, Percentage of lineages with and without isolated representatives in Bacteria and Archaea, based on 31 major lineages described previously[29]. The results highlight the massive scale of as-yet little-investigated biology in these domains. Archaeal Cas9 and the novel CRISPR–CasY were found exclusively in lineages with no isolated representatives. **b**, Locus organization of the discovered CRISPR–Cas systems.

[1]Department of Earth and Planetary Sciences, University of California, Berkeley, California 94720, USA. [2]Department of Molecular and Cell Biology, University of California, Berkeley, California 94720, USA. [3]Department of Chemistry, University of California, Berkeley, California 94720, USA. [4]Howard Hughes Medical Institute, University of California, Berkeley, California 94720, USA. [5]Innovative Genomics Initiative, University of California, Berkeley, California 94720, USA. [6]MBIB Division, Lawrence Berkeley National Laboratory, Berkeley, California 94720, USA. [7]Department of Environmental Science, Policy, and Management, University of California, Berkeley, California 94720, USA.
*These authors contributed equally to this work.

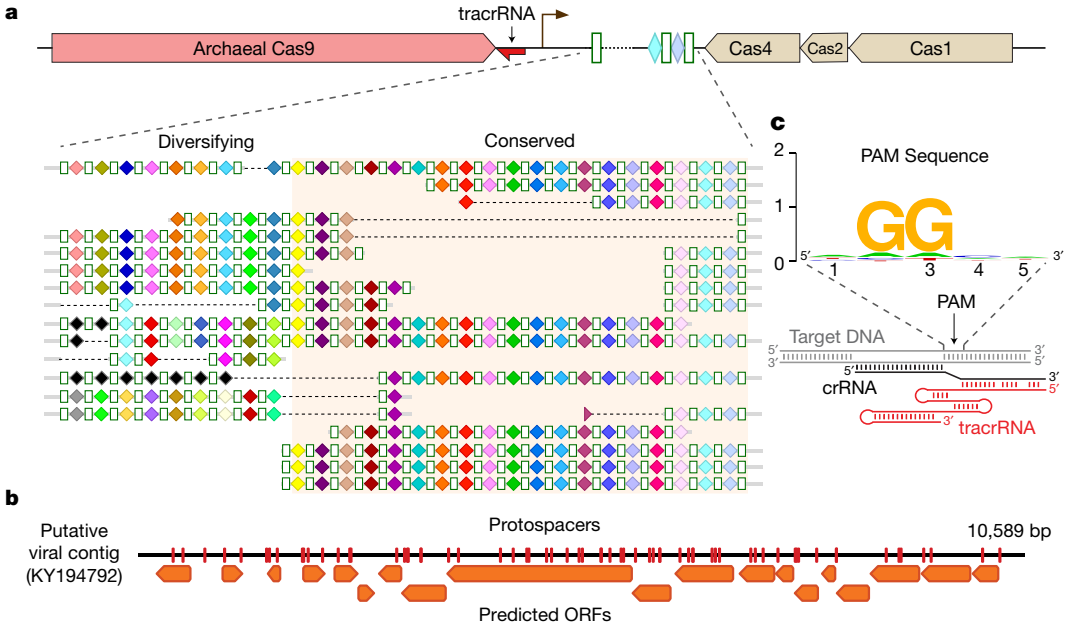

Figure 2 | ARMAN-1 CRISPR array diversity and identification of the ARMAN-1 Cas9 PAM sequence. a, CRISPR arrays reconstructed from AMD samples. White boxes indicate repeats, coloured diamonds indicate spacers (identical spacers are similarly coloured; unique spacers are black). The conserved region of the array is highlighted. The diversity of recently acquired spacers (on the left) indicates that the system is active. Analysis of within-population CRISPR variability is presented in Extended Data Fig. 2. **b**, A single circular, putative viral contig contains 56 protospacers (red vertical bars) from the ARMAN-1 CRISPR arrays. **c**, Sequence analysis of 240 protospacers (Supplementary Table 1) revealed a conserved 'NGG' PAM downstream of the protospacers. ORF, open reading frame.

with type II-B systems[3,11], yet the Cas9 sequence is more similar to type II-C proteins (Extended Data Fig. 4, Supplementary Data 3). Thus, the archaeal type II system may have arisen as a fusion of type II-C and II-B systems (Extended Data Fig. 3b).

Of the spacers of the ARMAN-1 CRISPR–Cas9 system, 56 target a 10-kbp circular sequence that encodes mostly short hypothetical proteins, and is probably an ARMAN-1 virus (Fig. 2b). Indeed, cryo-electron tomographic reconstructions have often identified viral particles attached to ARMAN cells[12,14]. ARMAN-1 protospacers also derived from a putative transposon within the genome of ARMAN-2 (another nanoarchaeon[13]) and a putative mobile element in the genomes of *Thermoplasmatales* archaea, including that of I-plasma[15] from the same ecosystem (Extended Data Fig. 5). Direct cytoplasmic 'bridges' were observed between ARMAN and *Thermoplasmatales* cells, implying a close relationship between them[12,14]. The ARMAN-1 CRISPR–Cas9 may therefore defend against transposon propagation between these organisms, a role that is reminiscent of piwi-interacting-RNA-mediated defence against transposition in the eukaryotic germ line[16].

Unlike the ARMAN-1 CRISPR–Cas system, the ARMAN-4 *cas9* gene has only one adjacent CRISPR repeat-spacer unit and no other *cas* genes in its vicinity (Extended Data Fig. 6). The lack of a typical CRISPR array and of *cas1* points to a system with no capacity to acquire additional spacers. No target could be identified for the spacer sequence, but given the conservation of the locus in samples collected over several years, we cannot rule out the possibility that it is functional as a 'single-target' CRISPR–Cas system. Conservation of a single spacer may indicate that the ARMAN-4 Cas9 exerts an alternative role, such as gene regulation[17] or involvement in cell–cell interactions[18].

Active DNA-targeting CRISPR–Cas systems use 2–4-nucleotide protospacer-adjacent motifs (PAMs) located next to target sequences for self-versus-non-self discrimination[19,20]. Examining sequences adjacent to the genomic target sequences revealed a strong 'NGG' PAM preference in ARMAN-1 (Fig. 2c). Cas9 also employs two separate transcripts, CRISPR RNA (crRNA) and trans-activating CRISPR RNA (tracrRNA), for RNA-guided DNA cleavage[21]. We identified a putative tracrRNA in the vicinity of both ARMAN-1 and ARMAN-4 CRISPR–Cas9 systems (Extended Data Fig. 7a–d). It has previously been suggested that type II CRISPR systems were absent from archaea owing to a lack of the host factor, RNase III, responsible for crRNA–tracrRNA guide complex maturation[11,22]. Notably, no RNase III homologues were identified in the ARMAN-1 genome (estimated to be 95% complete) and no internal promoters have been predicted for the CRISPR array[23], suggesting an as-yet-undetermined mechanism of guide RNA production. Biochemical experiments to test the cleavage activity of ARMAN-1 and ARMAN-4 Cas9 proteins purified from both *E. coli* and yeast did not reveal any detectable activity, nor did *in vivo E. coli*-targeting assays (see Extended Data Table 2 and Extended Data Fig. 7e–g). Given the unique physiology and ecological niche of these nanoarchaea, the lack of activity may be due to a post-translational modification or a co-factor absent from the experimental expression systems.

In addition to Cas9, only three families of class 2 Cas effector proteins have been discovered and experimentally validated: Cpf1, C2c1, and C2c2 (refs 4, 24, 25). Another gene, *c2c3*, which was identified only on small DNA fragments, has been suggested to encode such a protein as well[4]. We hypothesized that other distinct types of effector protein might exist within uncultivated microbes whose genomes were reconstructed from our metagenomic datasets. Indeed, a new type of class 2 CRISPR–Cas system was found in the genomes of two bacteria recovered from groundwater and sediment samples[26]. This system includes Cas1, Cas2, Cas4 and an uncharacterized protein of approximately 980 amino acids that we refer to as CasX. The high conservation (68% protein sequence identity; Supplementary Data 1) of this protein in two organisms belonging to different phyla, Deltaproteobacteria and Planctomycetes, suggests a recent cross-phylum transfer[27,28]. The CRISPR arrays associated with each CasX had highly similar repeats (86% identity) of 37 nucleotides, spacers of 33–34 nucleotides and a putative tracrRNA between the Cas operon and the CRISPR array (Fig. 1b, Extended Data Table 1). BLAST (https://blast.ncbi.nlm.nih.gov/Blast.cgi) searches revealed only weak similarity ($e > 1 \times 10^{-4}$) to transposases, with similarity restricted to specific regions of the CasX C terminus. Distant homology detection and protein modelling identified a RuvC domain near the CasX C-terminal end, with organization reminiscent of that found in type V CRISPR–Cas systems (Extended

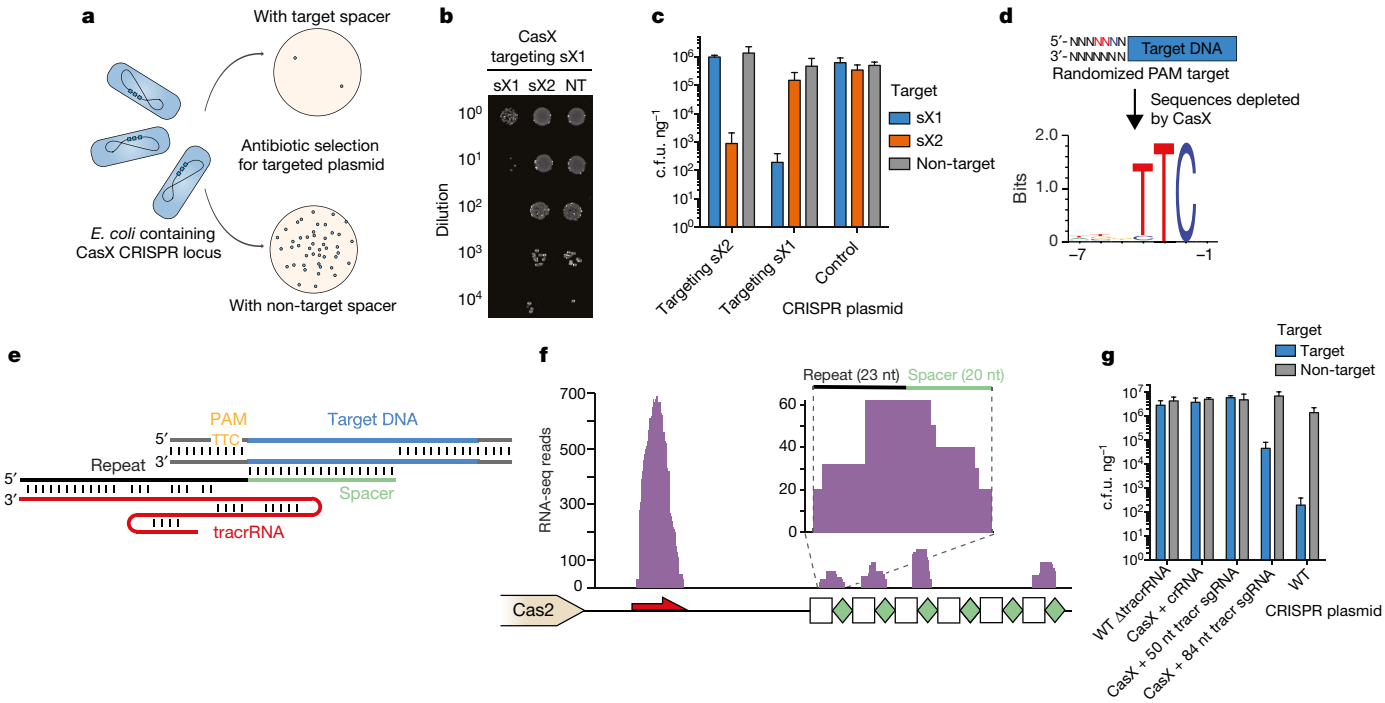

Figure 3 | CRISPR–CasX is a dual-guided system that mediates programmable DNA interference in *E. coli*. **a**, Diagram of CasX plasmid interference assays. **b**, Serial dilution of *E. coli* expressing the Planctomycetes CasX locus with spacer 1 (sX1) and transformed with the specified target. NT, non-target; sX1, CasX protospacer 1; sX2, CasX protospacer 2. **c**, Plasmid interference by Deltaproteobacteria CasX, using the same spacers and targets as in **b**. **d**, PAM depletion assays for the Planctomycetes CasX locus expressed in *E. coli*. Sequence logo was generated from PAM sequences depleted more than 30-fold compared to a control library (see also Extended Data Fig. 8). **e**, Diagram of CasX DNA interference. **f**, Mapping of environmental RNA sequences to the CasX CRISPR locus. Inset shows a detailed view of mapping to first repeat and spacer. Red arrow, putative tracrRNA; white boxes, repeats; green diamonds, spacers. **g**, Plasmid interference assays with the putative tracrRNA knocked out of the CasX locus, CasX coexpressed with a crRNA alone, a truncated sgRNA or a full-length sgRNA. Experiments in **c** and **g** were conducted in triplicate and mean ± s.d. is shown.

Data Fig. 3c). The rest of the CasX protein (630 N-terminal amino acids) showed no detectable similarity to any known protein, suggesting this is a novel class 2 effector. The combination of tracrRNA and separate Cas1, Cas2 and Cas4 proteins is unique among type V systems, and phylogenetic analyses indicate that the Cas1 from the CRISPR–CasX system is distant from those of any other known type V Cas (Extended Data Fig. 3a). Furthermore, CasX is considerably smaller than any known type V proteins: 980 amino acids compared to a typical size of approximately 1,200 amino acids for Cpf1, C2c1 and C2c3.

To test whether CasX is capable of RNA-guided DNA targeting, analogous to that by Cas9 and Cpf1 proteins, we synthesized a plasmid encoding a minimal CRISPR–CasX locus including *casX*, a short repeat-spacer array and intervening non-coding regions. We found that when it was expressed in *E. coli*, this minimal locus blocked transformation by a plasmid bearing a target sequence that we had identified by metagenomic analysis (Fig. 3a–c and Extended Data Fig. 8a, b). Furthermore, interference with transformation occurred only when the spacer sequence in the mini-locus matched the protospacer sequence in the plasmid target.

To identify a PAM sequence for CasX, we repeated the transformation assay in *E. coli* using a plasmid containing either a 5′ or 3′ randomized sequence adjacent to the target site. This analysis revealed a stringent preference for the sequence 'TTCN' located 5′ of the protospacer sequence (Fig. 3d). No 3′ PAM preference was observed (Extended Data Fig. 8c, d). Consistent with this finding, we observed that 'TTCA' is the sequence found upstream of the putative Deltaproteobacteria CRISPR–CasX protospacer that was identified in the environmental samples. Notably, both CRISPR–CasX loci share the same PAM sequence, in line with their high degree of protein sequence homology.

Examples of both single-RNA- and dual-RNA-guided systems exist among type V CRISPR loci. We used environmental RNA (metatranscriptomic) data to determine whether CasX requires a tracrRNA for DNA targeting activity. This analysis revealed a non-coding RNA transcript with sequence complementarity to the CRISPR repeat encoded between the Cas2 open reading frame and the CRISPR array (Fig. 3e, f). To check for expression of this non-coding RNA in *E. coli* expressing the CasX locus, we performed northern blots targeted against this transcript in both directions (Extended Data Fig. 8e, f). The results showed expression of a transcript of approximately 110 nucleotides encoded on the same strand as the *casX* gene, with a more heterogeneous transcript of around 60–70 nucleotides, suggesting that the leader sequence for the CRISPR array lies between the tracrRNA and the array. Transcriptomic mapping further suggests that the crRNA is processed to include around 23 nucleotides of the repeat and 20 nucleotides of the adjacent spacer, similar to the crRNA processing that occurs in CRISPR–Cas9 systems[21,22] (Fig. 3f). To determine whether CasX activity depends on the putative tracrRNA, we deleted this region from the minimal CRISPR–CasX locus described above, and repeated the plasmid interference assays. Deletion of the putative tracrRNA-encoding sequence from the CasX plasmid abolished robust transformation interference (Fig. 3g). This putative tracrRNA was joined with the processed crRNA using a tetraloop to form a single-guide RNA (sgRNA)[21]. Although expression using a heterologous promoter of the crRNA alone or a shortened version of the sgRNA did not produce any pronounced plasmid interference, expression of the full-length sgRNA conferred resistance to plasmid transformation (Fig. 3g). Together, these results establish CasX as a functional DNA-targeting, dual-RNA-guided CRISPR-associated protein.

We identified another new class 2 Cas protein encoded in the genomes of certain candidate phyla radiation bacteria[6,29] (Fig. 1, Extended Data Table 1). These bacteria typically have small cell sizes, very small genomes and a limited biosynthetic capacity[6,30–32], indicating

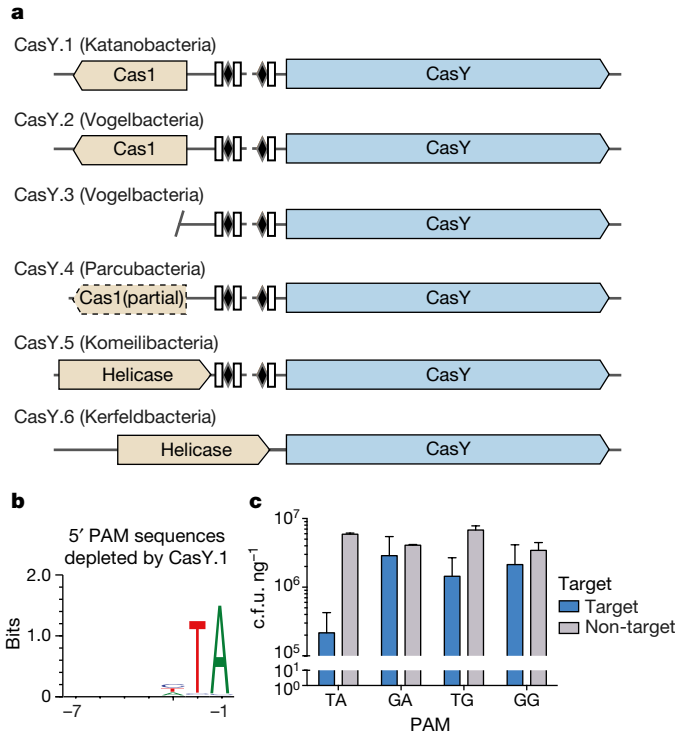

Figure 4 | Expression of a CasY locus in *E. coli* is sufficient for DNA interference. a, Diagrams of CasY loci and neighbouring proteins. **b**, Sequence logo of the 658 5′ PAM sequences depleted greater than threefold by CasY relative to a control library. **c**, Plasmid interference by *E. coli* expressing CasY.1 and CRISPR array expressed with a heterologous promoter and transformed with targets containing the indicated PAM. Experiments were conducted in triplicate and mean ± s.d. is shown.

that they are most likely to be symbionts[6,30–33]. The approximately 1,200 amino acid Cas protein, which we named CasY, appears to be part of a minimal CRISPR–Cas system that includes Cas1 and a CRISPR array (Fig. 4a). Most of the CRISPR arrays have unusually short spacers of 17–19 nucleotides, but one system, which lacks Cas1 (CasY.5), has longer spacers (27–29 nucleotides). No predicted tracrRNA was detected in the vicinity of CRISPR–CasY, based on partial complementarity to the repeat sequences; however, we had insufficient metatranscriptomic data mapped to the CasY loci to detect potential tracrRNA sequences. Thus, from the available data, we cannot exclude the possibility that CasY dependss on a tracrRNA for robust interference.

The six examples of CasY proteins that we identified had no significant sequence similarity to any protein in public databases. A sensitive search using profile Hidden Markov Models (HMMs)[34] built from published Cas proteins[3,4] indicated that four of the six CasY proteins had local similarities (*e* values $4 \times 10^{-11} - 3 \times 10^{-18}$) to C2c3 in the C-terminal region overlapping the RuvC domains and a small region (around 45 amino acids) of the N-terminal region (Extended Data Fig. 3c). The remaining two CasY proteins had no significant similarity to C2c3 proteins, despite sharing significant sequence similarity (best BLAST hits: $e = 6 \times 10^{-85}$, 7×10^{-75}) with the other CasY proteins (Supplementary Data 2). C2c3 proteins are putative type V Cas effectors[4] that were identified on short contigs with no taxonomic affiliation, and have not been validated experimentally. Strikingly, both CRISPR–CasY and C2c3 were found next to arrays with short spacers and within loci lacking Cas2, a protein considered essential for integrating DNA into the CRISPR array[9,35]. It remains to be seen whether these type V systems are functional for spacer acquisition.

Given the low homology of CRISPR–CasY to any experimentally validated CRISPR loci, we wondered whether this system confers RNA-guided DNA interference; however, owing to the short spacer length, we did not have reliable information about a possible PAM motif that might be required for such activity. To overcome this, we synthesized the entire CRISPR–CasY.1 locus with a shortened CRISPR array and introduced it into *E. coli* on a plasmid vector. These cells were then challenged in a transformation assay using a target plasmid with a sequence that matched a spacer in the array and contained an adjacent randomized 5′ or 3′ region to identify a possible PAM. Analysis of transformants revealed depletion of sequences containing a 5′ TA directly adjacent to the targeted sequence (Fig. 4b). On the basis of the identified PAM sequence, the CasY.1 locus was overexpressed using a heterologous promoter and tested against plasmids containing single PAMs. Plasmid interference was strongest in the presence of a target containing the identified 5′ TA PAM sequence (Fig. 4c). Thus, we conclude that CRISPR–CasY has DNA interference activity.

The systems described here are some of the most compact CRISPR–Cas loci identified to date and are found exclusively in metagenomic datasets. The small number of proteins that are required for interference and their relatively short length make these systems of particular relevance to the development of genome editing tools. Some of these compact loci were identified in organisms with very small genomes and, as a consequence of their small genome size, these organisms probably depend on other community members for basic metabolic requirements, meaning that they have largely remained outside the scope of traditional cultivation-based methods. For CasX and CasY, genomic context is critical for predicting functions that are not evident from unassembled sequence information. Furthermore, the identification of a putative tracrRNA, as well as targeted sequences uncovered through analysis of the genome-resolved metagenomic data, helped to guide functional testing. Notably, we show that metagenomic discoveries related to CRISPR–Cas systems are not restricted to *in silico* observations, but can be introduced into an experimental setting in which their activity can be analysed. Given that virtually all environments where life exists can now be probed by metagenomic methods, we anticipate that the combined computational–experimental approach will greatly expand the diversity of known CRISPR–Cas systems, enabling the development of new technologies for biological research and clinical applications.

Online Content Methods, along with any additional Extended Data display items and Source Data, are available in the online version of the paper; references unique to these sections appear only in the online paper.

Received 28 October; accepted 16 December 2016.
Published online 22 December 2016.

1. Barrangou, R. *et al.* CRISPR provides acquired resistance against viruses in prokaryotes. *Science* **315,** 1709–1712 (2007).
2. Sorek, R., Kunin, V. & Hugenholtz, P. CRISPR—a widespread system that provides acquired resistance against phages in bacteria and archaea. *Nat. Rev. Microbiol.* **6,** 181–186 (2008).
3. Makarova, K. S. *et al.* An updated evolutionary classification of CRISPR–Cas systems. *Nat. Rev. Microbiol.* **13,** 722–736 (2015).
4. Shmakov, S. *et al.* Discovery and functional characterization of diverse class 2 CRISPR–Cas systems. *Mol. Cell* **60,** 385–397 (2015).
5. Barrangou, R. & Doudna, J. A. Applications of CRISPR technologies in research and beyond. *Nat. Biotechnol.* **34,** 933–941 (2016).
6. Brown, C. T. *et al.* Unusual biology across a group comprising more than 15% of domain Bacteria. *Nature* **523,** 208–211 (2015).
7. Sharon, I. & Banfield, J. F. Genomes from metagenomics. *Science* **342,** 1057–1058 (2013).
8. Levy, A. *et al.* CRISPR adaptation biases explain preference for acquisition of foreign DNA. *Nature* **520,** 505–510 (2015).
9. Yosef, I., Goren, M. G. & Qimron, U. Proteins and DNA elements essential for the CRISPR adaptation process in *Escherichia coli*. *Nucleic Acids Res.* **40,** 5569–5576 (2012).
10. Nuñez, J. K., Lee, A. S. Y., Engelman, A. & Doudna, J. A. Integrase-mediated spacer acquisition during CRISPR–Cas adaptive immunity. *Nature* **519,** 193–198 (2015).
11. Chylinski, K., Makarova, K. S., Charpentier, E. & Koonin, E. V. Classification and evolution of type II CRISPR–Cas systems. *Nucleic Acids Res.* **42,** 6091–6105 (2014).
12. Baker, B. J. *et al.* Enigmatic, ultrasmall, uncultivated Archaea. *Proc. Natl Acad. Sci. USA* **107,** 8806–8811 (2010).
13. Baker, B. J. *et al.* Lineages of acidophilic Archaea revealed by community genomic analysis. *Science* **314,** 1933–1935 (2006).

14. Comolli, L. R. & Banfield, J. F. Inter-species interconnections in acid mine drainage microbial communities. *Front. Microbiol*. **5,** 367 (2014).
15. Yelton, A. P. *et al.* Comparative genomics in acid mine drainage biofilm communities reveals metabolic and structural differentiation of co-occurring archaea. *BMC Genomics* **14,** 485 (2013).
16. Vagin, V. V. *et al.* A distinct small RNA pathway silences selfish genetic elements in the germline. *Science* **313,** 320–324 (2006).
17. Stern, A., Keren, L., Wurtzel, O., Amitai, G. & Sorek, R. Self-targeting by CRISPR: gene regulation or autoimmunity? *Trends Genet*. **26,** 335–340 (2010).
18. Zegans, M. E. *et al.* Interaction between bacteriophage DMS3 and host CRISPR region inhibits group behaviors of *Pseudomonas aeruginosa*. *J. Bacteriol*. **191,** 210–219 (2009).
19. Shah, S. A., Erdmann, S., Mojica, F. J. M. & Garrett, R. A. Protospacer recognition motifs: mixed identities and functional diversity. *RNA Biol*. **10,** 891–899 (2013).
20. Anders, C., Niewoehner, O., Duerst, A. & Jinek, M. Structural basis of PAM-dependent target DNA recognition by the Cas9 endonuclease. *Nature* **513,** 569–573 (2014).
21. Jinek, M. *et al.* A programmable dual-RNA-guided DNA endonuclease in adaptive bacterial immunity. *Science* **337,** 816–821 (2012).
22. Deltcheva, E. *et al.* CRISPR RNA maturation by trans-encoded small RNA and host factor RNase III. *Nature* **471,** 602–607 (2011).
23. Zhang, Y., Rajan, R., Seifert, H. S., Mondragón, A. & Sontheimer, E. J. DNase H Activity of *Neisseria meningitidis* Cas9. *Mol. Cell* **60,** 242–255 (2015).
24. Zetsche, B. *et al.* Cpf1 is a single RNA-guided endonuclease of a class 2 CRISPR–Cas system. *Cell* **163,** 759–771 (2015).
25. Abudayyeh, O. O. *et al.* C2c2 is a single-component programmable RNA-guided RNA-targeting CRISPR effector. *Science* **353,** aaf5573 (2016).
26. Anantharaman, K. *et al.* Thousands of microbial genomes shed light on interconnected biogeochemical processes in an aquifer system. *Nat. Commun*. **7,** 13219 (2016).
27. Godde, J. S. & Bickerton, A. The repetitive DNA elements called CRISPRs and their associated genes: evidence of horizontal transfer among prokaryotes. *J. Mol. Evol.* **62,** 718–729 (2006).
28. Burstein, D. *et al.* Major bacterial lineages are essentially devoid of CRISPR-Cas viral defence systems. *Nat. Commun*. **7,** 10613 (2016).
29. Hug, L. A. *et al.* A new view of the tree of life. *Nat. Microbiol*. **1,** 16048 (2016).
30. Luef, B. *et al.* Diverse uncultivated ultra-small bacterial cells in groundwater. *Nat. Commun*. **6,** 6372 (2015).
31. Kantor, R. S. *et al.* Small genomes and sparse metabolisms of sediment-associated bacteria from four candidate phyla. *MBio* **4,** e00708–e00713 (2013).
32. Nelson, W. C. & Stegen, J. C. The reduced genomes of Parcubacteria (OD1) contain signatures of a symbiotic lifestyle. *Front. Microbiol*. **6,** 713 (2015).
33. Rinke, C. *et al.* Insights into the phylogeny and coding potential of microbial dark matter. *Nature* **499,** 431–437 (2013).
34. Finn, R. D., Clements, J. & Eddy, S. R. HMMER web server: interactive sequence similarity searching. *Nucleic Acids Res*. **39,** W29–W37 (2011).
35. Nuñez, J. K. *et al.* Cas1–Cas2 complex formation mediates spacer acquisition during CRISPR–Cas adaptive immunity. *Nat. Struct. Mol. Biol*. **21,** 528–534 (2014).

Supplementary Information is available in the online version of the paper.

Acknowledgements We thank N. Ma, K. Zhou and D. McGrath for technical assistance; C. Brown, M. Olm, M. O'Connell, J. Chen and S. Floor for reading the manuscript and discussions; and V. Yu for the *S. cerevisiae* expression strain. D.B. was supported by a long-term EMBO fellowship, L.B.H. by a US National Science Foundation Graduate Research Fellowship, and A.J.P. by a fellowship of the German Science Foundation (DFG PR 1603/1-1). J.A.D. is an Investigator of the Howard Hughes Medical Institute. This research was supported in part by the Allen Distinguished Investigator Program, through The Paul G. Allen Frontiers Group, the National Science Foundation (MCB-1244557 to J.A.D.) and the Lawrence Berkeley National Laboratory's Sustainable Systems Scientific Focus Area funded by the US Department of Energy (DE-AC02-05CH11231 to J.F.B.). DNA sequencing was conducted at the DOE Joint Genome Institute, a DOE Office of Science User Facility, via the Community Science Program.

Author Contributions D.B., L.B.H., S.C.S., J.A.D. and J.F.B. designed the study and wrote the manuscript. A.J.P., K.A., J.F.B., B.T.C. and D.B. assembled the data and reconstructed the genomes. D.B., L.B.H., S.C.S. and J.F.B. computationally analysed the CRISPR–Cas systems. L.B.H. and D.B. designed and executed experimental work with CRISPR–CasX and CRISPR–CasY. S.C.S. designed and executed the experimental work with ARMAN Cas9. The manuscript was read, edited and approved by all authors.

Author Information Reprints and permissions information is available at www.nature.com/reprints. The authors declare competing financial interests: details are available in the online version of the paper. Readers are welcome to comment on the online version of the paper. Correspondence and requests for materials should be addressed to J.F.B. (jbanfield@berkeley.edu) or J.A.D. (doudna@berkeley.edu).

Reviewer Information *Nature* thanks E. Sontheimer, R. Sorek and M. White for their contribution to the peer review of this work.

METHODS

No statistical methods were used to predetermine sample size. The experiments were not randomized and the investigators were not blinded to allocation during experiments and outcome assessment.

Metagenomics and metatranscriptomics. Metagenomic samples from three different sites were analysed: (1) AMD samples collected between 2006 and 2010 from the Richmond Mine, Iron Mountain, California[36,37]. (2) Groundwater and sediment samples collected between 2007 and 2013 from the Rifle Integrated Field Research (IFRC) site, adjacent to the Colorado River near Rifle, Colorado[6,26]. (3) Groundwater collected in 2009 and 2014 from Crystal Geyser, a cold, CO_2-driven geyser on the Colorado Plateau in Utah[38].

For the AMD data, DNA extraction methods and short read sequencing were as described[36,37]. For the Rifle data, DNA extraction, sequencing, assembly and genome reconstruction were as described[6,26]. For samples from Crystal Geyser, methods were as described[38,39]. Rifle metatranscriptomic data were used from ref. 6.

In brief, DNA was extracted from samples using the PowerSoil DNA Isolation Kit (MoBio Laboratories Inc.). RNA was extracted from 0.2-μm filters collected from six 2011 Rifle groundwater samples. Following RNA extraction using the Invitrogen TRIzol reagent, DNA was removed with the Qiagen RNase-Free DNase Set and Qiagen Mini RNeasy kits, and cDNA template library was generated using the Applied Biosystems SOLiD Total RNA-Seq kit. DNA was sequenced on Illumina HiSeq2000 platform, and Metatrancriptomic cDNA on 5500XL SOLiD platform after emulsion clonal bead amplification using the SOLiD EZ Bead system (Life Technologies). For the Crystal Geyser data and reanalysis of the AMD data, sequences were assembled using IDBA-UD[40]. DNA and RNA (cDNA) read-mapping used to determine sequencing coverage and gene expression, respectively, was performed using Bowtie2 (ref. 41). Open reading frames were predicted on assembled scaffolds using Prodigal[42]. Scaffolds from the Crystal Geyser dataset were binned on the basis of differential coverage abundance patterns using a combination of ABAWACA[6], ABAWACA2 (https://github.com/CK7), Maxbin2 (ref. 43), and tetranucleotide frequency using Emergent Self-Organizing Maps (ESOM)[44]. Genomes were manually curated using per cent GC content, taxonomic affiliation and genome completeness. Scaffolding errors were corrected using ra2.py (https://github.com/christophertbrown).

CRISPR–Cas computation analyses. The assembled contigs from the various samples were scanned for known Cas proteins using hidden Markov model (HMM) profiles, which were built using the HMMer suite[34], based on alignments from refs 3, 4. CRISPR arrays were identified using a local version of the CrisprFinder software[45]. Loci that contained both Cas1 and a CRISPR array were further analysed if one of the ten open reading frames adjacent to the *cas1* gene encoded for an uncharacterized protein larger than 800 amino acids, and no known *cas* interference genes were identified on the same contig. These large proteins were further analysed as potential class 2 Cas effectors. The potential effectors were clustered to protein families based on sequence similarities using MCL[46]. These protein families were expanded by building HMMs representing each of these families, and using them to search the metagenomic datasets for similar Cas proteins. To compare the identified protein families to known proteins, homologues were searched using BLAST[47] against the NCBI non-redundant (nr) and metagenomic (env_nr) protein databases, as well as HMM searches against the UniProt KnowledegeBase[34,48]. Only proteins with no full-length hits (>25% of the protein's length) were considered novel proteins. Distant homology searches of the putative Cas proteins were performed using HHpred from the HH-suite[49]. High scoring HHpred hits were used to infer domain architecture based on comparison to solved crystal structures[50,51], and secondary structure that was predicted by JPred4 (ref. 52). Protein modelling was performed using Phyre2 (ref. 53). The HMM database, including the newly discovered Cas proteins, is available in Supplementary Data 6.

Spacer sequences were determined from the assembled data using CrisprFinder[45]. CRASS[54] was used to locate additional spacers in short DNA reads of the relevant samples. Spacer targets (protospacers) were then identified by BLAST[47] searches (using 'task blastn-short') against the relevant metagenomic assemblies for hits with ≤1 mismatch to spacers. Hits belonging to contigs that contained an associated repeat were filtered out (to avoid identifying CRISPR arrays as protospacers). Protospacer adjacent motifs (PAMs) were identified by aligning regions flanking the protospacers and visualized using WebLogo[55]. In cases where one spacer had multiple putative protospacers with different compositions of flanking nucleotides, each distinct combination of protospacer and downstream nucleotides was taken into account for the logo calculation. RNA structures were predicted using mFold[56]. Average nucleotide identity was computed with the pyani Python module (https://github.com/widdowquinn/pyani), using the Mummer[57] method. CRISPR array diversity was analysed by manually aligning spacers, repeats and flanking sequences from the assembled data. Manual alignments and contig visualizations were performed with Geneious 9.1.

For the phylogenetic analyses of Cas1 and Cas9, we used proteins of the newly identified systems along with the proteins from refs 3, 4. A non-redundant set was compiled by clustering together proteins with ≥90% identity using CD-HIT[58]. Alignments were produced with MAFFT[59], and maximum-likelihood phylogenies were constructed using RAxML[60] with PROTGAMMALG as the substitution model and 100 bootstrap samplings. Cas1 tree were rooted using the branch leading to casposons. Trees were visualized using FigTree 1.4.1 (http://tree.bio.ed.ac.uk/software/figtree/) and iTOL v3(ref. 61).

Generation of heterologous plasmids. Metagenomic contigs were made into minimal CRISPR interference plasmids by removing proteins associated with acquisition for CRISPR–CasX and reducing the size of the CRISPR array for both CRISPR–CasX and CRISPR–CasY. The minimal locus was synthesized as Gblocks (Integrated DNA Technology). Native promoters were used, with the exception of the overexpression of CasY.1 and expression of the crRNA alone or sgRNA for CasX in Fig. 3g where the J23119 constitutive promoter was used. The minimal CRISPR loci were assembled using Gibson Assembly[62] into a plasmid with a p15A origin of replication and chloramphenicol resistance gene. Detailed plasmid maps are available at the links provided in Supplementary Table 2.

PAM depletion assay. PAM depletion assays were conducted as previously described[63] with modification. Plasmid libraries containing randomized PAM sequences were assembled by annealing a DNA oligonucleotide containing a target with a 7-nucleotide randomized PAM region with a primer (Supplementary Table 2) and extended with Klenow Fragment (NEB). The double-stranded DNA was digested with EcoRI and NcoI and ligated into a pUC19 backbone. The ligated library was transformed into *E. coli* DH5α and $>10^8$ cells were harvested and the plasmids extracted and purified. We transformed 200 ng of the pooled library into electrocompetent *E. coli* harbouring a CRISPR locus or a control plasmid with no locus. The transformed cells were plated on selective medium containing carbenicillin (100 mg l^{-1}) and chloramphenicol (30 mg l^{-1}) for 30 h at 25 °C. Plasmid DNA was extracted and the PAM sequence was amplified with adapters for Illumina sequencing. The 7-nucleotide PAM region was extracted and PAM frequencies calculated for each 7-nucleotide sequence. PAM sequences depleted above the specified threshold were used to generate a sequence logo with WebLogo[55].

Plasmid interference. Putative targets identified from metagenomic sequence analysis or PAM depletion assays were cloned into a pUC19 plasmid. We transformed 10 ng of target plasmid into electrocompetent *E. coli* (NEB Stable) containing the CRISPR loci plasmid. CasX.1 was used for the plasmid interference assays under control of native promoters or using a strong heterologous promoter (J23119) for sgRNA and crRNA expression. CasY.1 was put under the control of a heterologous promoter (J23119) for these assays. Cells were recovered for 2 h at 25 °C in super optimal broth and an appropriate dilution was plated on selective media. Plates were incubated at 25 °C and colony forming units were counted. All plasmid interference experiments were performed in triplicate and electrocompetent cells were prepared independently for each replicate.

Northern blots. *E. coli* containing the deltaproteobacteria CasX CRISPR locus was grown to $A_{600} = 1$ at 25 °C in super optimal broth. RNA was extracted by warm phenol extraction, separated on 10% denaturing polyacrylamide gel and blotted as previously described[64].

ARMAN-Cas9 protein expression and purification. Expression constructs for Cas9 from ARMAN-1 (AR1) and ARMAN-4 (AR4) were assembled from gBlocks (Integrated DNA Technologies) that were codon-optimized for *E. coli*. The assembled genes were cloned into a pET-based expression vector as an N-terminal His_6-MBP or His_6 fusion protein. Expression vectors were transformed into BL21(DE3) *E. coli* cells and grown in LB broth at 37 °C. For protein expression, cells were induced during mid-log phase with 0.4 mM IPTG (isopropyl β-D-1-thiogalactopyranoside) and incubated overnight at 16 °C. All subsequent steps were conducted at 4 °C. Cell pellets were resuspended in lysis buffer (50 mM Tris-HCl, 500 mM NaCl, 1 mM TCEP, 10 mM Imidazole, 0.5% Triton X-100; pH 8) and supplemented with Complete protease inhibitor mixture (Roche) before lysis by sonication. Lysate was clarified by centrifugation at 15,000*g* for 40 min and applied to Superflow Ni-NTA agarose (Qiagen) in batch. The resin was washed extensively with wash buffer A (50 mM Tris-HCl, 500 mM NaCl, 1 mM TCEP, 10 mM imidazole; pH 8) followed by 5 column volumes of wash buffer B (50 mM Tris-HCl, 1 M NaCl, 1 mM TCEP, 10 mM imidazole; pH 8). Protein was eluted off of Ni-NTA resin with elution buffer (50 mM Tris-HCl, 500 mM NaCl, 1 mM TCEP, 300 mM Imidazole; pH 8). The His_6-MBP tag was removed by TEV protease during overnight dialysis against wash buffer A. Cleaved Cas9 was removed from the affinity tag through a second Ni-NTA agarose column. The protein was dialysed into IEX buffer A (50 mM Tris-HCl, 300 mM NaCl, 1 mM TCEP, 5% glycerol; pH 7.5) before application to a 5-ml Heparin HiTrap column (GE Life Sciences). Cas9 was eluted over a linear NaCl (0.3–1.5 M) gradient. Fractions were pooled and concentrated with a 30-kDa spin concentrator (Thermo Fisher). When applicable, Cas9 was further purified via size-exclusion chromatography on a Superdex

200-pg column (GE Life Sciences) and stored in IEX buffer A for subsequent cleavage assays. For yeast expression, AR1-Cas9 was cloned into a Gal1/10 His6-MBP TEV Ura *S. cerevisiae* expression vector (Addgene plasmid 48305). The vector was transformed into a BY4741 URA3 strain and cultures were grown in synthetic media (5 g l^{-1} ammonium sulfate, 1.7 g l^{-1} nitrogen base (Sunrise Science), 0.72 g l^{-1} complete supplement mixture – ura (Sunrise Science), 20 g l^{-1} glucose, 1.5% glycerol, 2% lactic acid) at 30 °C. At an A_{600} of approximately 0.6, protein expression was induced with 2% (w/v) galactose and incubated overnight at 16 °C. Protein purification was performed as above.

RNA *in vitro* transcription and oligonucleotide purification. *In vitro* transcription reactions were performed as previously described[65] using synthetic DNA templates containing a T7 promoter sequence. All *in vitro* transcribed putative guide RNA sequences and target RNA or DNA were purified via denaturing PAGE. Double-stranded target RNA and DNA were hybridized in 20 mM Tris HCl (pH 7.5) and 100 mM NaCl by incubation at 95 °C for 1 min, followed by slow-cooling to room temperature. Hybrids were purified by native PAGE. RNA and DNA sequences used in this study are listed in Supplementary Table 2.

***In vitro* cleavage assays.** Purified DNA and RNA oligonucleotides were radiolabelled using T4 polynucleotide kinase (NEB) and [γ-32P] ATP (Perkin-Elmer) in 1× PNK buffer for 30 min at 37 °C. PNK was heat inactivated at 65 °C for 20 min and free ATP was removed from the labelling reactions using illustra Microspin G-25 columns (GE Life Sciences). CrRNA and tracrRNA were mixed in equimolar quantities in 1× refolding buffer (50 mM Tris HCl pH 7.5, 300 mM NaCl, 1 mM TCEP, 5% glycerol) and incubated at 70 °C for 5 min and then slow-cooled to room temperature. The reactions were supplemented to 1 mM final metal concentration and subsequently heated at 50 °C for 5 min. After slow-cooling to room temperature, refolded guides were placed on ice. Unless noted for buffer or salt concentration, Cas9 was reconstituted with an equimolar amount of guide in 1× cleavage buffer (50 mM Tris HCl pH 7.5, 300 mM NaCl, 1 mM TCEP, 5% glycerol, 5 mM divalent metal) at 37 °C for 10 min. Cleavage reactions were conducted in 1× cleavage buffer with a 10× excess of Cas9-guide complex over radiolabelled target at 37 °C or the indicated temperature. Reactions were quenched in an equal volume of gel loading buffer supplemented with 50 mM EDTA. Cleavage products were resolved on 10% denaturing PAGE and visualized by phosphorimaging.

***In vivo E. coli* interference assays.** *E. coli* transformation assays for ARMAN-1 Cas9 and ARMAN-4 Cas9 were conducted as previously published[66]. Briefly, *E. coli* transformed with plasmids expressing guide RNA sequences were made electrocompetent. Cells were then transformed with 9 fmol of plasmid encoding wild-type or catalytically inactive Cas9 (dCas9). A dilution series of recovered cells was plated on LB plates with selective antibiotics. Colonies were counted after 16 h at 37 °C.

Data Availability. All the sequences reported in this study for the first time have been deposited in NCBI database under BioProject PRJNA349044. The NCBI Nucleotide database accession and coordinates of each locus are specified in Extended Data Table 1. The BioSample and Sequence Reads Archive (SRA) accessions for the ARMAN-1 spacers and protospacers are detailed in Supplementary Table 1. The HMMs used in this study are provided in Supplementary Data 6. All other data are available from the authors upon reasonable request.

36. Denef, V. J. & Banfield, J. F. *In situ* evolutionary rate measurements show ecological success of recently emerged bacterial hybrids. *Science* **336,** 462–466 (2012).
37. Miller, C. S., Baker, B. J., Thomas, B. C., Singer, S. W. & Banfield, J. F. EMIRGE: reconstruction of full-length ribosomal genes from microbial community short read sequencing data. *Genome Biol.* **12,** R44 (2011).
38. Probst, A. J. *et al.* Genomic resolution of a cold subsurface aquifer community provides metabolic insights for novel microbes adapted to high CO_2 concentrations. *Environ. Microbiol.* http://dx.doi.org/10.1111/1462-2920.13362 (2016).
39. Emerson, J. B., Thomas, B. C., Alvarez, W. & Banfield, J. F. Metagenomic analysis of a high carbon dioxide subsurface microbial community populated by chemolithoautotrophs and bacteria and archaea from candidate phyla. *Environ. Microbiol.* **18,** 1686–1703 (2016).
40. Peng, Y., Leung, H. C. M., Yiu, S. M. & Chin, F. Y. L. IDBA-UD: a *de novo* assembler for single-cell and metagenomic sequencing data with highly uneven depth. *Bioinformatics* **28,** 1420–1428 (2012).
41. Langmead, B. & Salzberg, S. L. Fast gapped-read alignment with Bowtie 2. *Nat. Methods* **9,** 357–359 (2012).
42. Hyatt, D. *et al.* Prodigal: prokaryotic gene recognition and translation initiation site identification. *BMC Bioinformatics* **11,** 119 (2010).
43. Wu, Y.-W., Simmons, B. A. & Singer, S. W. MaxBin 2.0: an automated binning algorithm to recover genomes from multiple metagenomic datasets. *Bioinformatics* **32,** 605–607 (2016).
44. Dick, G. J. *et al.* Community-wide analysis of microbial genome sequence signatures. *Genome Biol.* **10,** R85 (2009).
45. Grissa, I., Vergnaud, G. & Pourcel, C. CRISPRFinder: a web tool to identify clustered regularly interspaced short palindromic repeats. *Nucleic Acids Res.* **35,** W52–W57 (2007).
46. Enright, A. J., Van Dongen, S. & Ouzounis, C. A. An efficient algorithm for large-scale detection of protein families. *Nucleic Acids Res.* **30,** 1575–1584 (2002).
47. Camacho, C. *et al.* BLAST+: architecture and applications. *BMC Bioinformatics* **10,** 421 (2009).
48. The UniProt Consortium. UniProt: a hub for protein information. *Nucleic Acids Res.* **43,** D204–D212 (2015).
49. Remmert, M., Biegert, A., Hauser, A. & Söding, J. HHblits: lightning-fast iterative protein sequence searching by HMM–HMM alignment. *Nat. Methods* **9,** 173–175 (2011).
50. Dong, D. *et al.* The crystal structure of Cpf1 in complex with CRISPR RNA. *Nature* **532,** 522–526 (2016).
51. Yamano, T. *et al.* Crystal structure of Cpf1 in complex with guide RNA and target DNA. *Cell* **165,** 949–962 (2016).
52. Drozdetskiy, A., Cole, C., Procter, J. & Barton, G. J. JPred4: a protein secondary structure prediction server. *Nucleic Acids Res.* **43** (W1), W389–W394 (2015).
53. Kelley, L. A., Mezulis, S., Yates, C. M., Wass, M. N. & Sternberg, M. J. E. The Phyre2 web portal for protein modeling, prediction and analysis. *Nat. Protocols* **10,** 845–858 (2015).
54. Skennerton, C. T., Imelfort, M. & Tyson, G. W. Crass: identification and reconstruction of CRISPR from unassembled metagenomic data. *Nucleic Acids Res.* **41,** e105(2013).
55. Crooks, G. E., Hon, G., Chandonia, J.-M. & Brenner, S. E. WebLogo: a sequence logo generator. *Genome Res.* **14,** 1188–1190 (2004).
56. Zuker, M. Mfold web server for nucleic acid folding and hybridization prediction. *Nucleic Acids Res.* **31,** 3406–3415 (2003).
57. Kurtz, S. *et al.* Versatile and open software for comparing large genomes. *Genome Biol.* **5,** R12 (2004).
58. Fu, L., Niu, B., Zhu, Z., Wu, S. & Li, W. CD-HIT: accelerated for clustering the next-generation sequencing data. *Bioinformatics* **28,** 3150–3152 (2012).
59. Katoh, K. & Standley, D. M. MAFFT multiple sequence alignment software version 7: improvements in performance and usability. *Mol. Biol. Evol.* **30,** 772–780 (2013).
60. Stamatakis, A. RAxML version 8: a tool for phylogenetic analysis and post-analysis of large phylogenies. *Bioinformatics* **30,** 1312–1313 (2014).
61. Letunic, I. & Bork, P. Interactive tree of life (iTOL) v3: an online tool for the display and annotation of phylogenetic and other trees. *Nucleic Acids Res.* **44** (W1), W242–W245 (2016).
62. Gibson, D. G. *et al.* Enzymatic assembly of DNA molecules up to several hundred kilobases. *Nat. Methods* **6,** 343–345 (2009).
63. Esvelt, K. M. *et al.* Orthogonal Cas9 proteins for RNA-guided gene regulation and editing. *Nat. Methods* **10,** 1116–1121 (2013).
64. Zhang, Y. *et al.* Processing-independent CRISPR RNAs limit natural transformation in *Neisseria meningitidis*. *Mol. Cell* **50,** 488–503 (2013).
65. Sternberg, S. H., Haurwitz, R. E. & Doudna, J. A. Mechanism of substrate selection by a highly specific CRISPR endoribonuclease. *RNA* **18,** 661–672 (2012).
66. Oakes, B. L. *et al.* Profiling of engineering hotspots identifies an allosteric CRISPR–Cas9 switch. *Nat. Biotechnol.* **34,** 646–651 (2016).
67. Jinek, M. *et al.* Structures of Cas9 endonucleases reveal RNA-mediated conformational activation. *Science* **343,** http://dx.doi.org/10.1126/science.1247997 (2014).

Extended Data Figure 1 | Multiple sequence alignment of newly described Cas9 proteins. Alignment of Cas9 proteins from ARMAN-1 and ARMAN-4, as well as two closely related Cas9 proteins from uncultivated bacteria, to the *Actinomyces naeslundii* Cas9, whose structure has been solved[67].

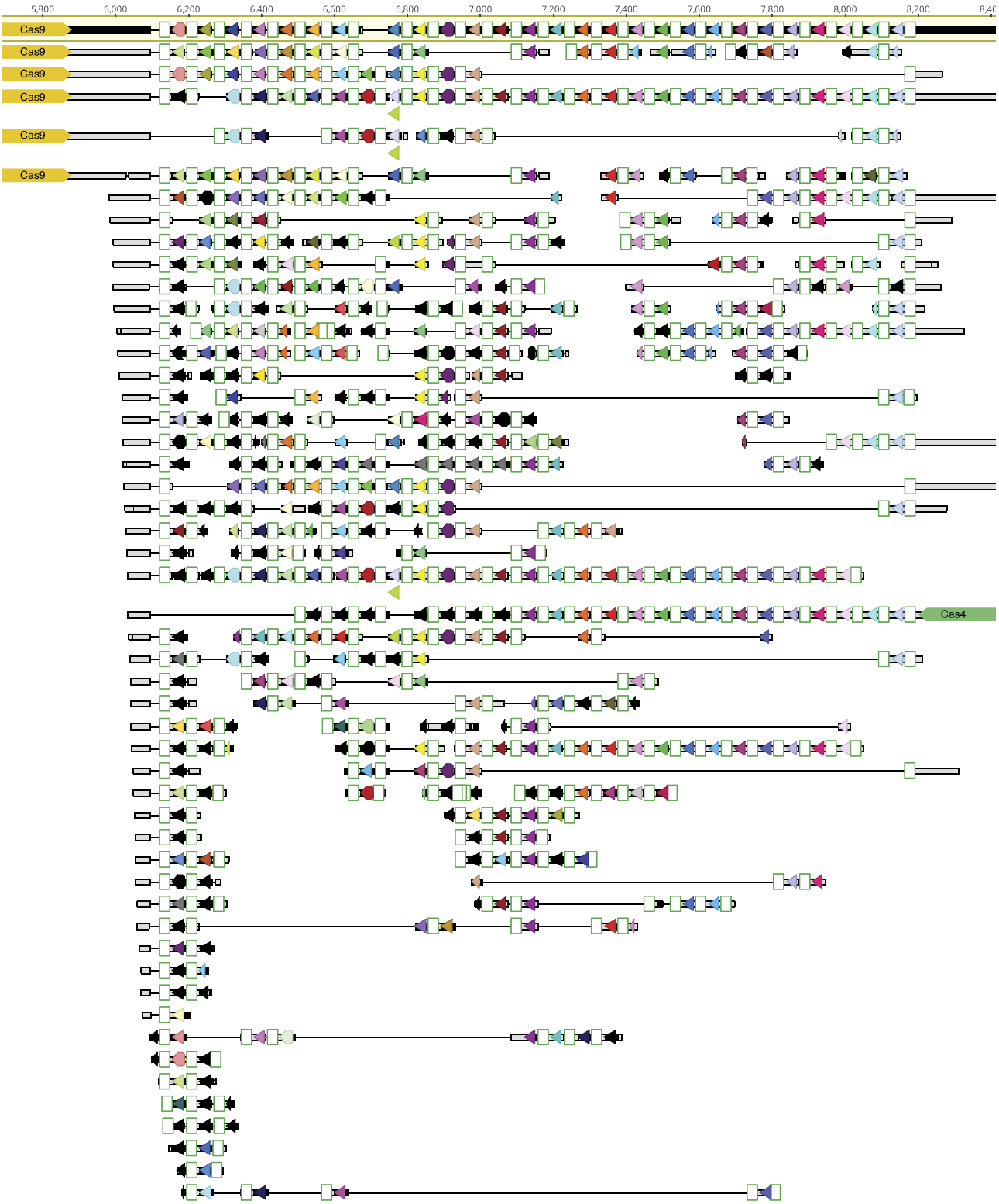

Extended Data Figure 2 | Within-population variability of ARMAN-1 CRISPR arrays. Variability of reconstructed CRISPR arrays, including the most well represented (and thus assembled) sequences (Fig. 2) and array segments representing locus variants that were reconstructed from the short DNA reads. Variability is due to spacers that were present in only a subset of archaeal cells in the population, as well as spacers whose context differed owing to spacer loss (indicated by black lines). White boxes indicate repeats and coloured arrows indicate CRISPR spacers (spacers with different colours have different sequences, except for unique spacers that are black). In CRISPR systems, spacers are typically added unidirectionally, so the high variety of spacers on the left side is attributed to recent acquisition.

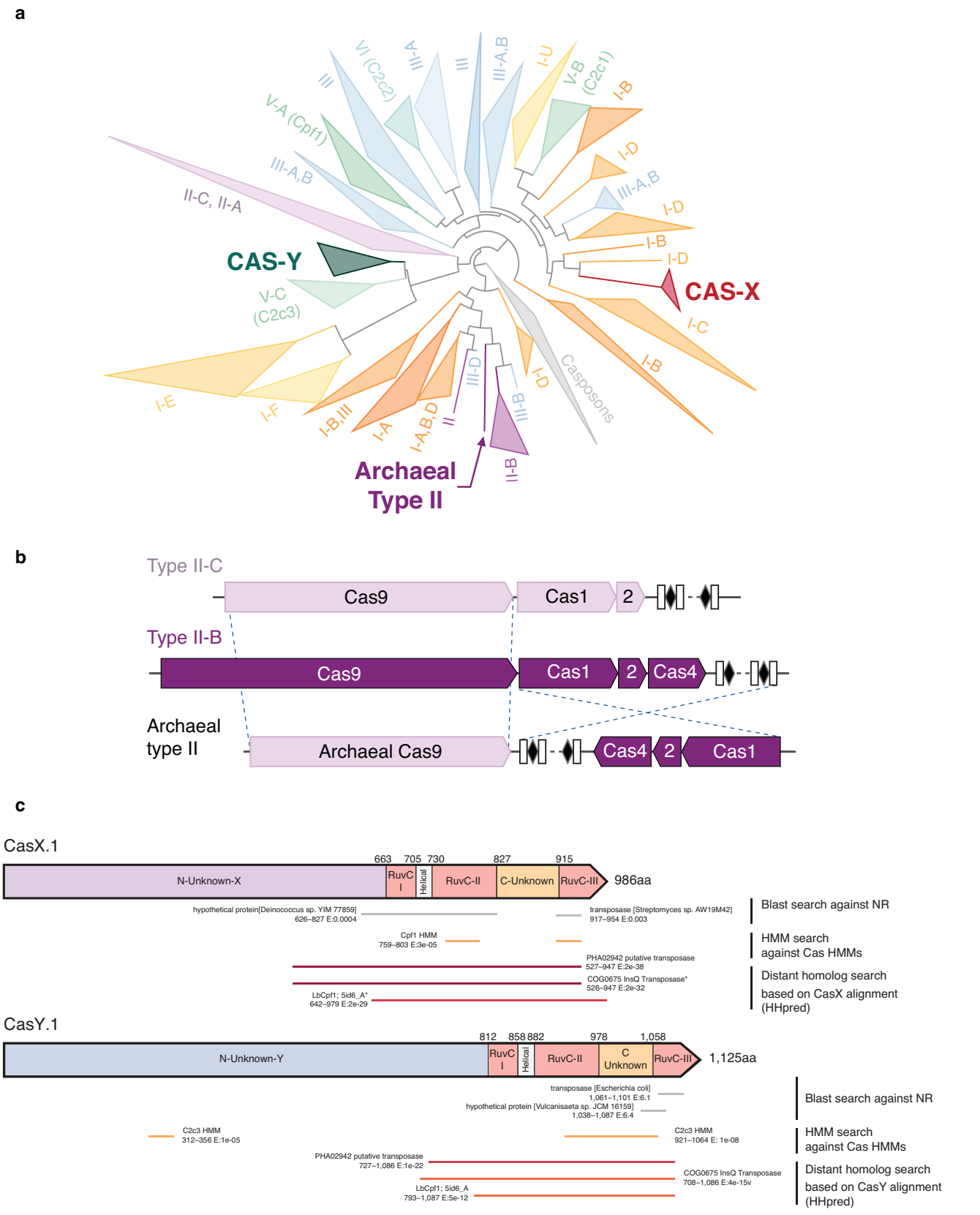

Extended Data Figure 3 | Novelty of the reported CRISPR–Cas systems. **a**, Simplified phylogenetic tree of the universal Cas1 protein. CRISPR types of known systems are noted on the wedges and branches; the newly described systems are in bold. Detailed Cas1 phylogeny is provided in Supplementary Data 4. **b**, Proposed evolutionary scenario that gave rise to the archaeal type II system as a result of a recombination between type II-B and type II-C loci. **c**, Similarity of CasX and CasY to known proteins based on the following searches: (1) BLAST search against the non-redundant (NR) protein database of NCBI; (2) HMM search against an HMM database of known Cas proteins; and (3) distant homology search using HHpred[49] (E, *e* value).

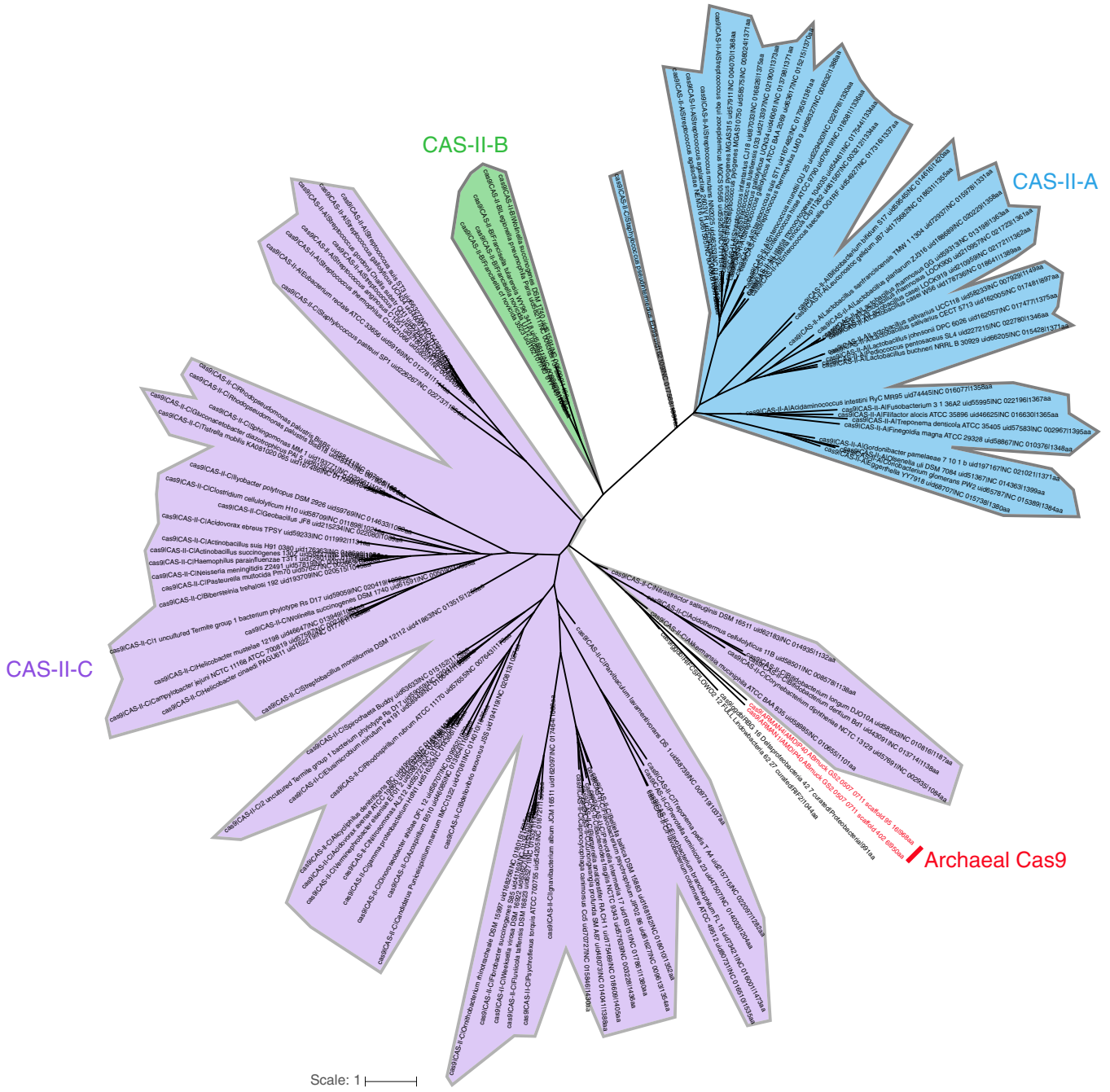

Extended Data Figure 4 | Evolutionary tree of Cas9 homologues. Maximum-likelihood phylogenic tree of Cas9 proteins, showing the previously described systems coloured based on their type. II-A, blue; II-B, green; II-C, purple. The archaeal Cas9 (red) cluster with type II-C CRISPR–Cas systems, together with two newly described bacterial Cas9 from uncultivated bacteria. A detailed tree is provided in Supplementary Data 5.

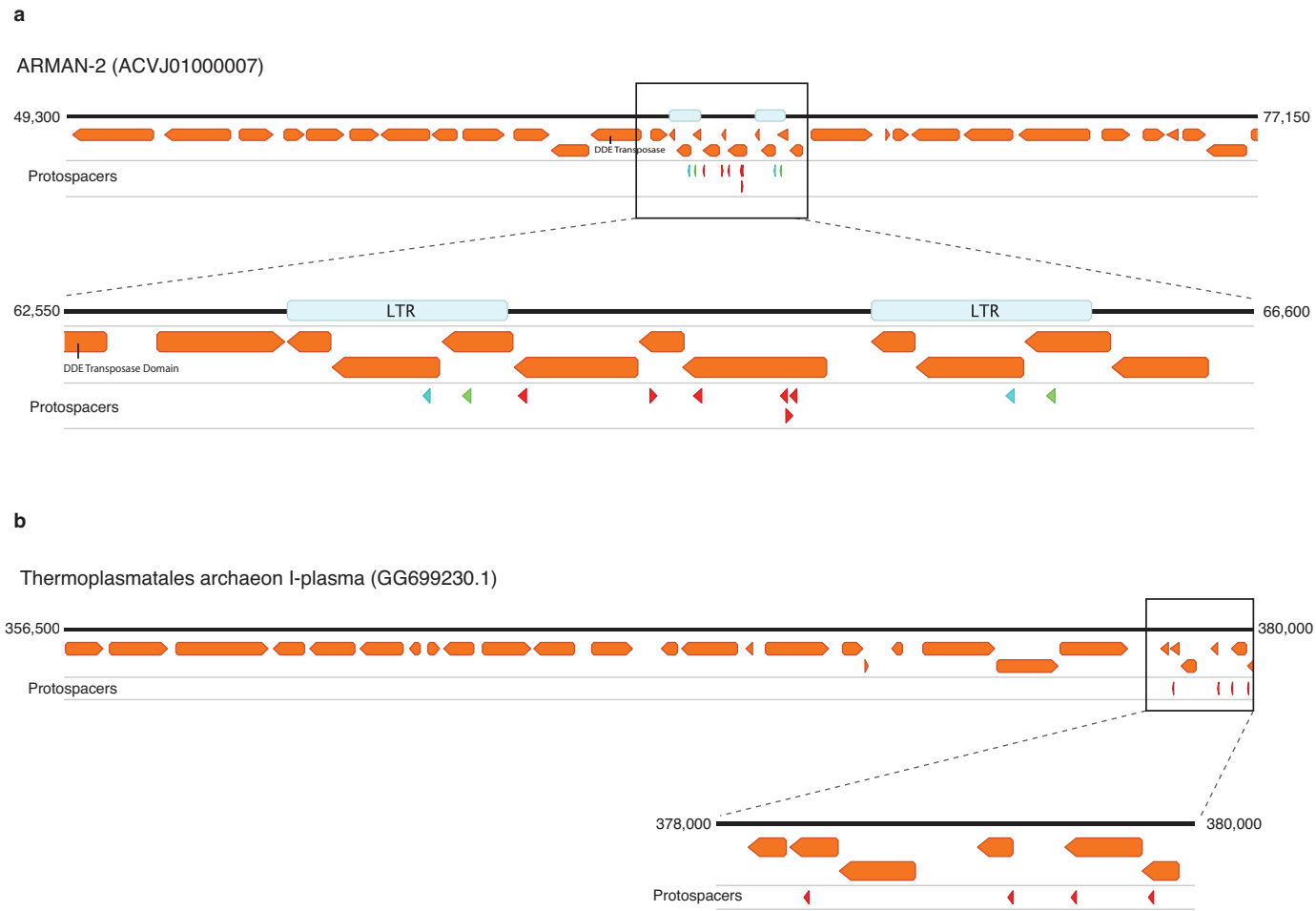

Extended Data Figure 5 | ARMAN-1 spacers map to genomes of archaeal community members. a, Protospacers from ARMAN-1 map to the genome of ARMAN-2, a nanoarchaeon from the same environment. Six protospacers (red arrowheads) map uniquely to a portion of the genome flanked by two long-terminal repeats (LTRs), and two additional protospacers match perfectly within the LTRs (blue and green arrowheads). This region is likely to be a transposon, suggesting that the CRISPR–Cas system of ARMAN-1 plays a role in suppressing mobilization of this element. **b**, Protospacers also map to a *Thermoplasmatales* archaeon (I-plasma), another member of the Richmond Mine ecosystem that is found in the same samples as ARMAN organisms. The protospacers cluster within a region of the genome encoding short, hypothetical proteins, suggesting this might also represent a mobile element. NCBI accession codes are provided in parentheses.

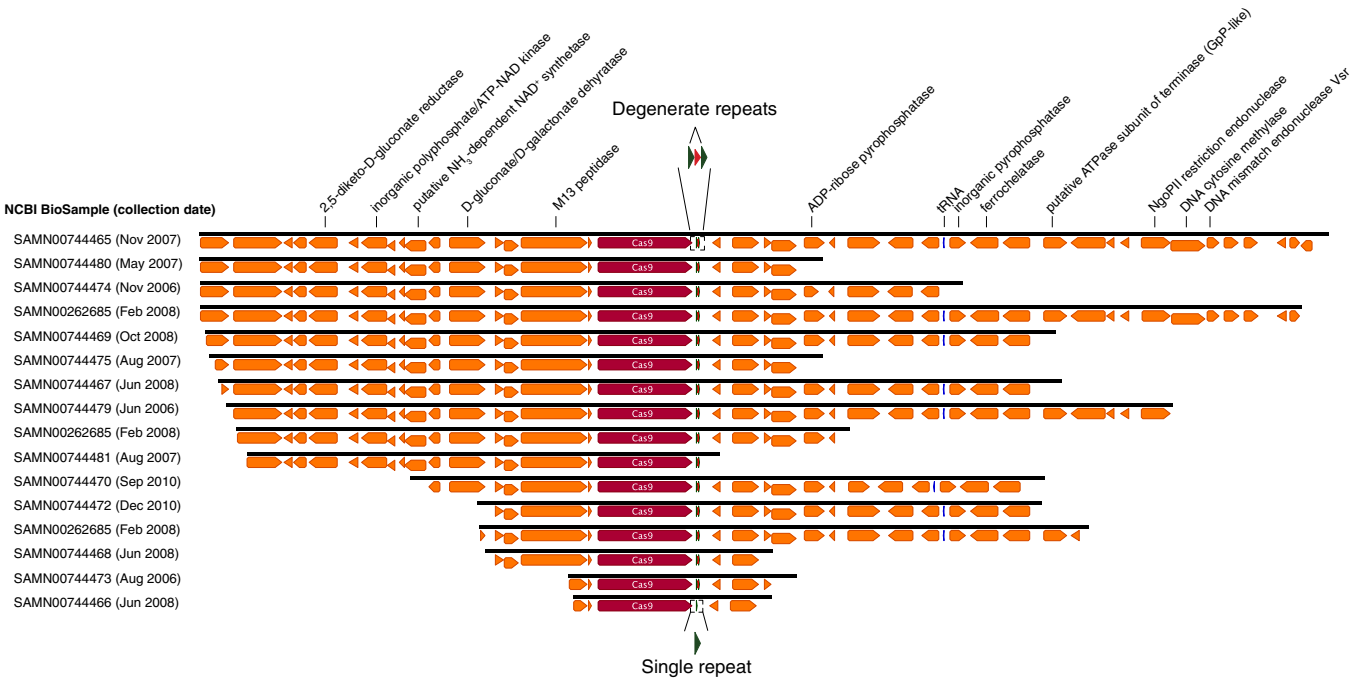

Extended Data Figure 6 | Archaeal Cas9 from ARMAN-4 with a degenerate CRISPR array is found on numerous contigs. Cas9 from ARMAN-4 is highlighted in dark red on 16 nearly identical contigs from different samples. Proteins with putative domains or functions are labelled, whereas hypothetical proteins are unlabelled. Fifteen of the contigs contain two degenerate direct repeats (36 nucleotides long with one mismatch) and a single conserved spacer of 36 nucleotides. The remaining contig contains only one direct repeat. Unlike ARMAN-1, no additional Cas proteins are found adjacent to Cas9 in ARMAN-4.

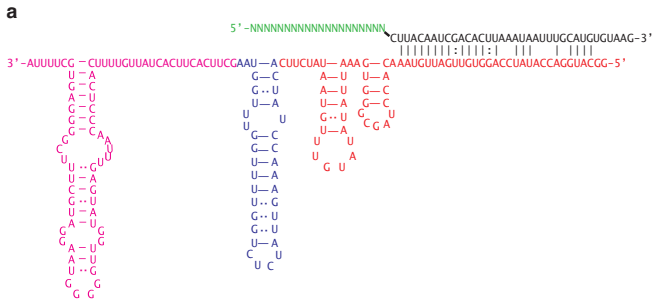

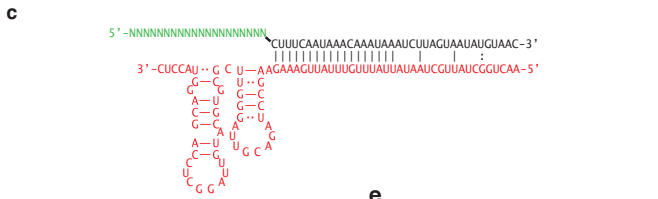

e

In vivo E. coli targeting assay

Protein	Guide
AR1-Cas9 AR1-dCas9	crRNA sgRNA-69 sgRNA-104 sgRNA-179
AR4-Cas9 AR4-dCas9	crRNA sgRNA-75 sgRNA-122

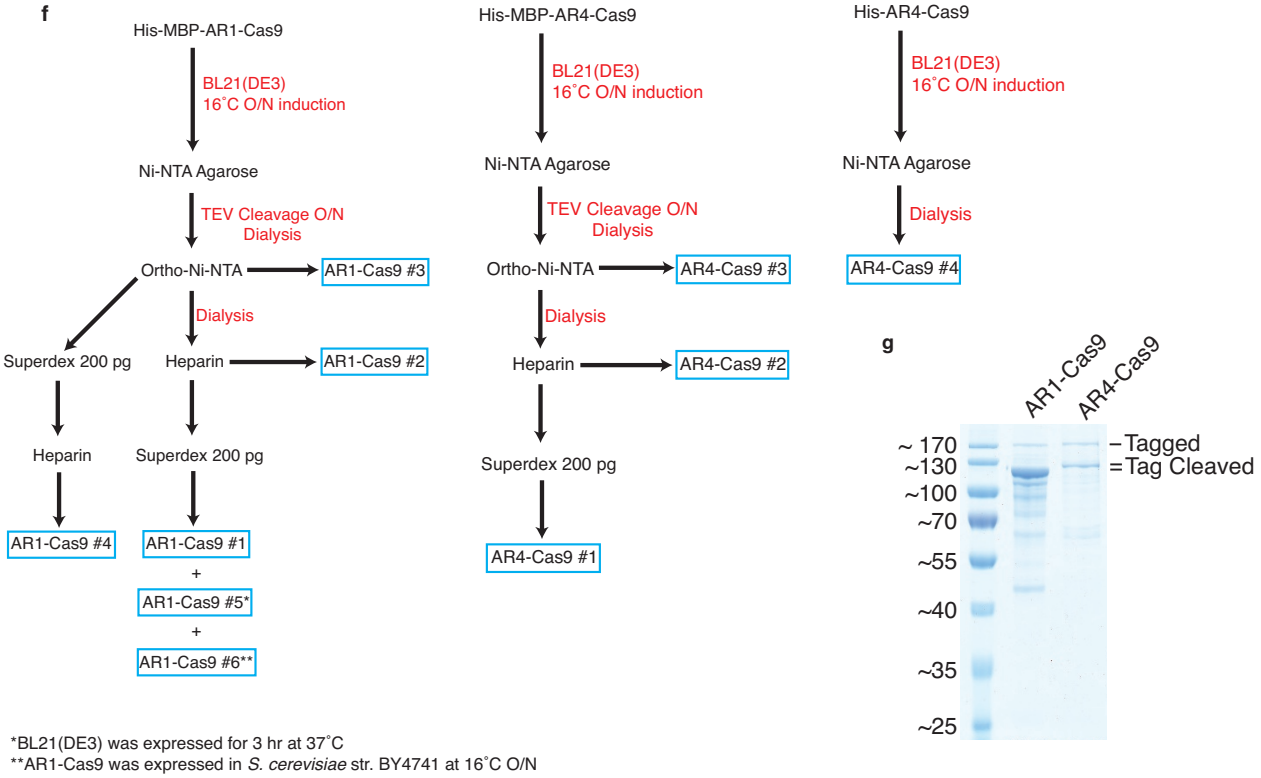

*BL21(DE3) was expressed for 3 hr at 37˚C
**AR1-Cas9 was expressed in *S. cerevisiae* str. BY4741 at 16˚C O/N

Extended Data Figure 7 | Predicted structures of guide RNA and purification schema for *in vitro* biochemistry studies. a, The CRISPR repeat and tracrRNA anti-repeat are depicted in black whereas the spacer-derived sequence is shown as a series of green Ns. No clear termination signal can be predicted from the locus, so three different tracrRNA lengths were tested based on their secondary structure: 69, 104, and 179 nucleotides in red, blue, and pink, respectively. **b**, Engineered single-guide RNA corresponding to dual-guide in **a**. **c**, Dual-guide RNA for ARMAN-4 Cas9 with two different hairpins on 3′ end of tracrRNA (75 and 122 nucleotides). **d**, Engineered single-guide RNA corresponding to dual-guide in **c**. **e**, Conditions tested in *E. coli in vivo* targeting assay. **f**, ARMAN-1 (AR1) and ARMAN-4 (AR4) Cas9 were expressed and purified under a variety of conditions as outlined in the Methods section. Proteins outlined in blue boxes were tested for cleavage activity *in vitro*. **g**, Fractions of AR1-Cas9 and AR4-Cas9 purifications were separated on a 10% SDS–PAGE gel.

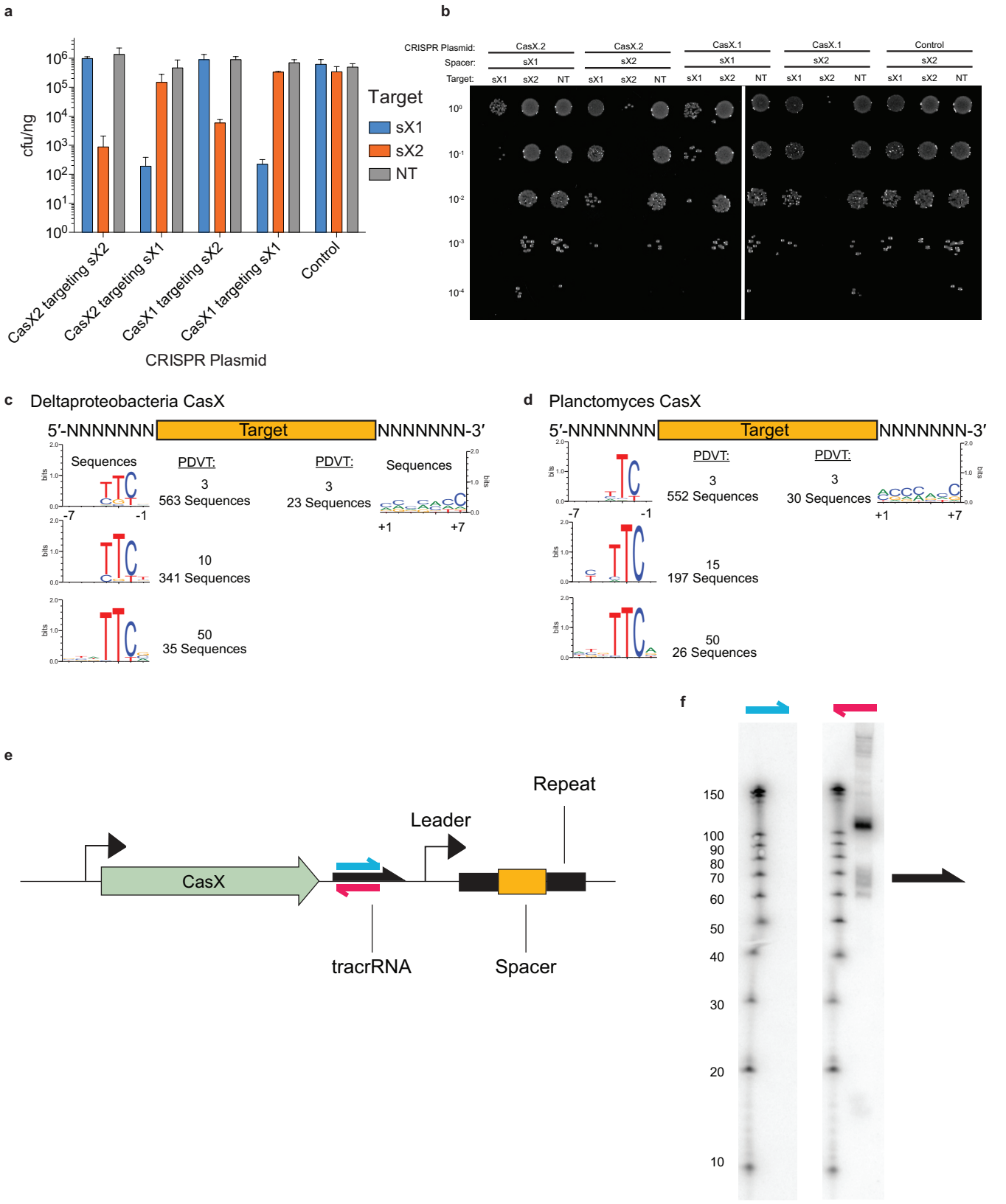

Extended Data Figure 8 | Programmed DNA interference by CasX. **a**, Plasmid interference assays for CasX.1 (Deltaproteobacteria) and CasX.2 (Planctomycetes), continued from Fig. 3c (sX1, CasX spacer 1; sX2, CasX spacer 2; NT, non-target). Experiments were conducted in triplicate and mean ± s.d. is shown. **b**, Serial dilution of *E. coli* expressing a CasX locus and transformed with the specified target, continued from Fig. 3b. **c**, PAM depletion assays for the Deltaproteobacteria CasX and **d**, Planctomycetes CasX expressed in *E. coli*. PAM sequences depleted greater than the indicated PAM depletion value threshold (PDVT) compared to a control library were used to generate the sequence logo. **e**, Diagram depicting the location of northern blot probes for CasX.1. **f**, Northern blots for CasX.1 tracrRNA in total RNA extracted from *E. coli* expressing the CasX.1 locus. The sequences of the probes used are provided in Supplementary Table 2.

Extended Data Table 1 | CRISPR–Cas loci identified in this study

Taxonomic group	Cas effector	NCBI Accession	Coordinates	Repeat length	# spacers	Spacers avg. length
ARMAN-1	Cas9	MOEG01000017	1827..7130	36	271	34.5
ARMAN-4	Cas9	KY040241	11779..14900	36	1	36
Deltaproteobacteria	CasX	MGPG01000094	4319..9866	37	5	33.6
Planctomycetes	CasX	MHYZ01000150	1..5586	37	7	32.3
Candidatus Katanobacteria	CasY.1	MOEH01000029	459..5716	26	14	17.1
Candidatus Vogelbacteria	CasY.2	MOEJ01000028	7322..13087	26	18	17.3
Candidatus Vogelbacteria	CasY.3	MOEK01000006	1..4657	26	12	17.3
Candidatus Parcubacteria	CasY.4	KY040242	1..5193	25	13	18.4
Candidatus Komeilibacteria	CasY.5	MOEI01000022	2802..7242	36	8	26
Candidatus Kerfeldbacteria	CasY.6	MHKD01000036	11503..15366	NA	NA	NA

Details regarding the organisms and genomic location in which the CRISPR–Cas system were identified, as well as information on the number and average length of reconstructed spacers and the repeat length. ARMAN-1 spacers were reconstructed from 16 samples, see details in Supplementary Table 1. NA, not available.

Extended Data Table 2 | *In vitro* cleavage conditions assayed for Cas9 from ARMAN-1 and ARMAN-4

Protein Purification	Buffer	Salt (mM)	Metal	Guide	Target	Temperature
AR1-Cas9 #1	Tris pH 7.5	300	Mg^{2+} Mn^{2+} Zn^{2+}	crRNA cr:69 cr:104 cr:179	dsDNA ssDNA DNA Bubble ssRNA dsDNA	37
AR1-Cas9 #1	Tris pH 7.5	100-500	Mg^{2+}	cr:69 cr:104 cr:179	dsDNA	37
AR1-Cas9 #1	Tris pH 7.5	300	Mg^{2+} Mn^{2+} Zn^{2+}	cr:69 cr:104 cr:179	dsDNA	30-48
AR1-Cas9 #1	MOPS: pH 6 pH 6.5 pH 7.0 pH 7.5	300	Mg^{2+}	cr:69 cr:104 cr:179	dsDNA	37
AR1-Cas9 #1	Citrate: pH 5 pH 5.5 pH 6	300	Mg^{2+}	cr:69 cr:104 cr:179	dsDNA	37
AR1-Cas9 #1	Tris pH 7.5	300	Mg^{2+} Mn^{2+} Zn^{2+}	cr:69 cr:104 cr:179	plasmid	37-50
AR1-Cas9 #2	Tris pH 7.5	300	Mg^{2+} Mn^{2+} Zn^{2+}	cr:69 cr:104 cr:179	dsDNA	37
AR1-Cas9 #3	Tris pH 7.5	300	Mg^{2+} Mn^{2+} Zn^{2+}	cr:69 cr:104 cr:179	dsDNA	37
AR1-Cas9 #4	Tris pH 7.5	300	Mg^{2+} Mn^{2+} Zn^{2+}	cr:69 cr:104 cr:179	dsDNA	37
AR1-Cas9 #5	Tris pH 7.5	300	Mg^{2+} Mn^{2+} Zn^{2+}	cr:69 cr:104 cr:179	dsDNA	37
AR1-Cas9 #6	Tris pH 7.5	300	Mg^{2+} Mn^{2+} Zn^{2+}	cr:69 cr:104 cr:179	ssDNA dsDNA	37
AR4-Cas9 #1	Tris ph7.5	300	Mg^{2+} Mn^{2+} Zn^{2+}	sgRNA-122	dsDNA	37
AR4-Cas9 #2	Tris ph7.5	300	Mg^{2+} Mn^{2+} Zn^{2+}	sgRNA-122	dsDNA	37
AR4-Cas9 #3	Tris ph7.5	300	Mg^{2+} Mn^{2+} Zn^{2+}	sgRNA-122	dsDNA	37
AR4-Cas9 #4	Tris ph7.5	300	Mg^{2+} Mn^{2+} Zn^{2+}	sgRNA-122	dsDNA	37